ORIGINAL PAPER

ELASTIC BACKSCATTERED CROSS-SECTIONS OF 14N(P, P_0)14N AT HIGH ANGLES

MOHAMED ELTAYEB M. EISA[1,2*], JOHAN ANDRE MARS[3,4], MUSTAFA J. ABUALREISH[5,6], MARWA L. WAREGH[7]

Manuscript received: 03.05.2020; Accepted paper: 10.08.2020; Published online: 30.09.2020.

Abstract. *The importance and present needs of proton cross-section data of nitrogen needed by the Ion Beam Analysis (IBA) community are briefly reviewed. Previous experimental data presently used for the theoretical determination of the proton cross-sections are discussed. The Azure code based on the R-matrix formalism was then used to evaluate the data and to determine the nitrogen cross-section in the previous and presently desired angular domain and energy region of interest. The experimental elastic backscattering cross-section data, as spectra, for back-scattering analysis determined at angles in the laboratory frame of reference, $\theta_{i,lab}$, of 165°, 170°, and 176° are presented.*

Keywords: *elastic proton backscattering; R-matrix formalism; Azure code.*

1. INTRODUCTION

Elastic backscattering spectrometry (EBS) [1, 2] has over the past years emerged as a valuable Ion Beam Analysis (IBA) technique for quantifying concentrations of light elements such as C, O and N [3, 4]. This is especially so in the instance of biological specimen matrices, which might be multi-layered. These specimens consist primarily of proteins, and in turn amino acids. Hence, any change in composition due to pathologies would be reflected in the composition of these light elements (and so also P and S). As an example, calmodulin tissue, with a molecular mass of 16,7 kDa, consists of C, H, O, N, P, S and Ca. In normal tissue, the percentage concentrations of these elements are 45.50, 7.55, 30.41, 13.95, 0.01, 2.19 and 0.78 respectively. However, after fibrosis the concentrations were 45.44, 7.19, 29.50, 15.14, 0.00, 2.00, 0.73 respectively.

[1] Northern Border University, Department of Physics, Arar, Kingdom of Saudi Arabia.
[2] Sudan University of Science & Technology, Department of Physics, Khartoum, Sudan.
[3] University of the Western Cape, Department of Medical Bioscience, Private Bag X17, 7535 Bellville, Republic of South Africa. E-mail: jmars@uwc.ac.za.
[4] Cape Peninsula University of Technology, Faculty of Health & Wellness Sciences, 7535 Bellville, Republic of South Africa. E-mail: marsja@cput.ac.za.
[5] Northern Border University, College of Science, Department of Chemistry, Arar City, Kingdom of Saudi Arabia. E-mail: mustjeed_2008@hotmail.com.
[6] Omdurman Islamic University, Faculty of Science &Technology, Department of Chemistry, Omdurman, Sudan.
[7] National Cancer Institute, Department of Microbiology & Haematology, 47474 Misurata, Libya. E-mail: marwa.waregh@yahoo.com.
[*] *Corresponding author:* memeisa@yahoo.com.

In the characterization of these types of biomedical tissues proton--induced X-ray emission (PIXE) has extensively been used, and as the principal technique. The two important reasons for using PIXE as the principal technique are 1) the ability to perform multi-elemental analysis with the technique (i.e., from Na to U), and 2) the standard-less nature of the technique in determining element concentrations. The disadvantages in using PIXE are that light elements cannot be determined with the technique since the emitted X-rays of the elements might be absorbed in the detector window [5, 6] and 2) the optimum proton beam energy for PIXE is 3.000 MeV [7] whereas for EBS, higher energies are preferable [1, 4]. It should be noted that scanning electron microscopy - could be applied for the composition analyses, but as with PIXE, layered structures cannot be analysed with this technique. Hence PIXE and BS are ideal techniques for analysis of biomedical specimens. For this reason, both the emitted X-rays and backscattered particles are normally analysed simultaneously in the same chamber [8], with the respective angles of the detectors to the incoming beam are independent of the two analysis techniques.

The optimum angle for BS is 180^o [1, 7]. This geometry is however improbable when considering the finite size of the detector. The maximum angle of the silicon surface barrier detector, used to detect backscattered particles, to the incident beam at the Materials Research Group, iThemba LABS is 176^o [8]. Proton backscattered cross section data at this angle and in the preferred E_i (2000, say, to 3000) were needed since literature search [3, 9-17], and the evaluation of these data by [18] has shown that these experimental cross sections did not exist and that in various energy range, E_i, there exist significant differences in the cross-sections. These differences are shown in Fig. 1.

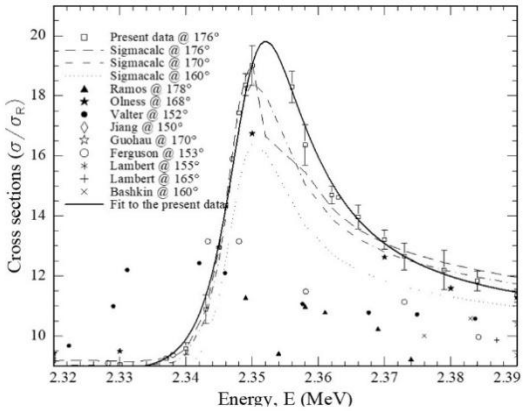

Figure 1. Illustration of the differences in cross-sections data for the reactions $^{14}N(p, p_0)^{14}N$ in the energy range E_i of 2320 to 2390 keV. The cross-sections data used in the comparison are those of [3,9-17]. The present data were obtained at θ_i of 176^o. The solid line is the fit to the present data using the Azure code [23].

Various analyses [19-21] and codes based on the R-matrix (scattering) theory or formalism (RMT) [22] have been applied in the evaluation of cross-sections of these codes, the Azure code has extensively been used in cross-sections' evaluation [23]. In this study the cross-sections were determined at three high angles, θ_i of 165^o, 170^o and 176^o. Improved cross-sections data are presented that could be applied in the determination of N concentration, especially for N determination in biological tissue.

2. MATERIALS AND METHODS

2.1. MATERIALS

Silicon deposited on iridium was used for standardisation of the backscattered particles. Metallic Si_3N_4 (Kyocera Advanced Ceramics, Kyoto, Japan) aș a standard, was used as target. The proton beam and energy were obtained with the 6 MeV Van de Graaff Accelerator in the Materials Research Department, at iThemba LABS, Faure, Rep. of South Africa [8]. Two analysis chambers, Backscattering chamber and Nuclear Microprobe chamber (BSc and NMPc) were used for experimentation. The angle of the detector mounting to the incoming beam of protons in the BSc was variable to a maximum angle of 170^o. Analysis of elastic backscattering at that angle and at 165^o were performed in that chamber. The detector resolution was 23 ± 2 keV and the solid angle 16 msr. In the NMPc the angle of the detector to the incoming beam of protons the target was fixed at 176^o. The detector had a resolution of 22 ± 2 keV. The distance from the specimen to detector was 16.3 ± 0.2 mm. A beam of α (^{4}He) particles was used to determine the standard stoichiometry. Afterwards, protons were used for bombardment.

2.2. METHODS

The beam energy was 1 MeV with an accuracy of 0.05%. The beam spot-size of 2.5μm×2.2μm was maintained. The total charge accumulated was 20000 pC. For the duration of the measurement, the vacuum in both chambers was 6.7×10^{-10} MPa. A current of 175±50 pA was maintained throughout the measurement sessions.

Based on the observed resonance anomalies (Table 1) in previous cross-sections data beam energy was varied from 2.000 MeV to 3.000 MeV at intervals of about 10 keV in regions where resonance anomalies were expected and about 50 keV otherwise.

Table 1. Compilation of the average energies of the resonance anomalies E_r for the reactions $^{14}N(p,p_0)^{14}N$ in the energy region, E_i, of 2000 to 3000 keV obtained from [3,14-17,24]. The excitation energy, E_x, in ^{15}O and the spin-parity assignment, J^π, were obtained from [25]. The regions indicated are those that concur with the regions in Fig. 1. EX is the extended region for the resonance of E_r of 3.209 MeV.

E_r (keV)	E_i (keV)	E_x (keV)	Γ(keV)	J^π	Regions
2348±7	2340-2360	9.49	12.0±4.5	$1/2^+$	C
2369±35	2355-2400	9.51	300±25	$1/2^+$	D
2480±3	2470-2490	9.61	10±5	$3/2^-$	E
2535±5	2530-2560	9.66	3±2	$7/2^+$	F
2600±50	2560-2615	9.72	1270±60	$1/2^+$ or $3/2^+$	G
3209±20	3180-3220	10.29	33±7	$5/2^+$	EX

3. RESULTS AND DISCUSSION

Seven regions of resonance changes were observed in the present cross-sections data. regions A and B are not accounted for in table 1 of the resonance anomalies. Region A could be considered as a non-resonance region, described as interference between isolated levels [22] and as (minima, two types and maxima, one type) parabolic. The anomaly, indicated by B in Fig. 1, could thus be described as a cross-section maxima. However, this anomaly is not present in IBANDL [2019, and data and references therein].

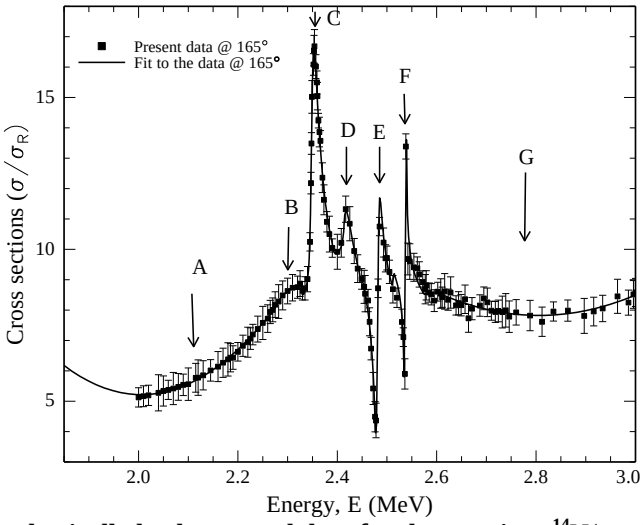

Figure 2. Spectrum of the elastically backscattered data for the reactions $^{14}N(p,p_0)^{14}N$ in the energy region E_i of 2000 to 3000 keV. The data were obtained at θ_i of 165°. The observed resonance regions and interference between levels are indicated.

The manufacturing company data did not state the chemical composition analysis and maintained that the standard is pure. It was surmised that O and/or H bonding might be present in the standard. Since the concentration would be very low, in ppm concentration range, it would not be observable in a scanning electron microscopy (SEM) spectrum since SEM MDL is 800 ppm [26]. The H would also not be determinable with Elastic Recoil Detection Analysis (ERDA) since the MDL is 500ppm [27]. For this reason, a Fourier transform infra-red (FTIR) analysis was performed. The FTIR spectrum is shown in Fig. 2.

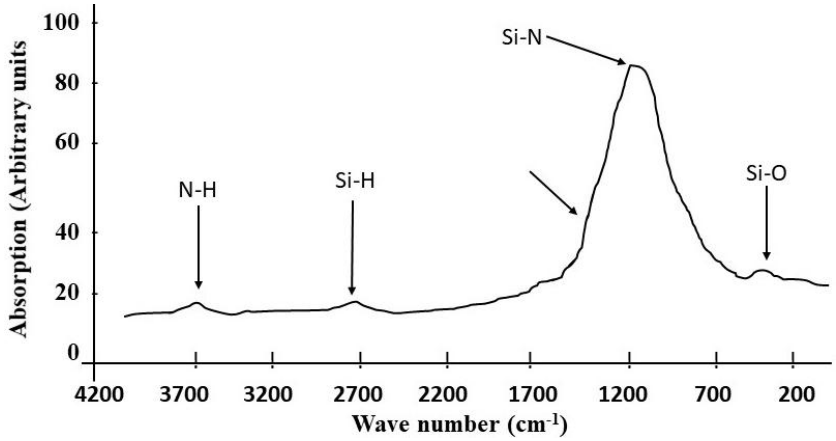

Figure 3. FTIR spectrum of the Si_3N_4 standard used in this study. The N-H, Si-H, the Si-N and the Si-O bonding are indicated. The N-O binding was not present. The arrow indicates the position of the Si-O binding should the O concentration had been relatively high.

For this reason, the resonance indicated by B in Fig. 1 was not evaluated. The cross-sections for the reactions $^{14}N(p, p_0)^{14}N$ in energy range E_i of 2340 to 2420 keV and for spin-parity of $J^\pi = 1/2^+$, are shown in Fig. 4. The cross-sections for the reactions $^{14}N(p, p_0)^{14}N$ in energy range 2.440 to 2.500 MeV for the spin-parity of $J^\pi = 1/2^+$, are shown in Fig. 5. The cross-sections for the reactions $^{14}N(p, p_0)^{14}N$ in energy range E_i of 2.500 to 2.560 MeV for spin-parity of $J^\pi = 3/2^-$ are shown in Fig. 6.

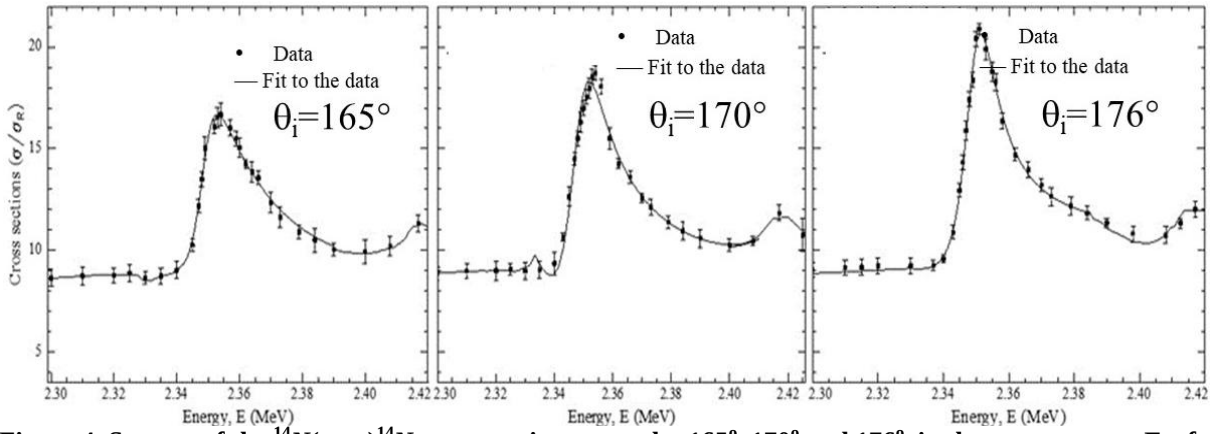

Figure 4. Spectra of the $^{14}N(p, p_0)^{14}N$ cross-sections at angles 165°, 170° and 176°, in the energy range E_i of 2340 to 2420 keV for the spin parity of J^{π} of $1/2^{+}$. Γ was 121±2 keV. E_r for the reactions was 2353±8 keV.

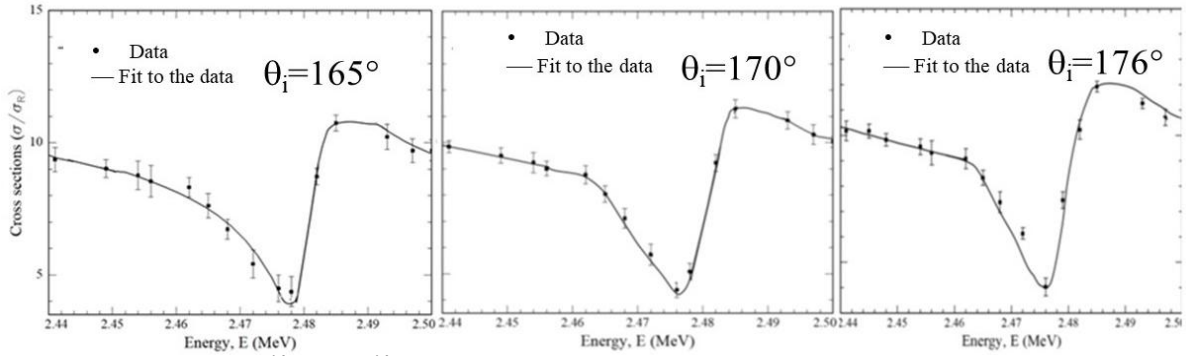

Figure 5. Spectra of the $^{14}N(p, p_0)^{14}N$ cross-sections at angles 165°, 170° and 176°, in the energy range 2440 to 2500 keV for the spin parity of J^{π} of $3/2^{-}$. Γ was 15±2 keV. E_r for the reactions was 2780±15 keV.

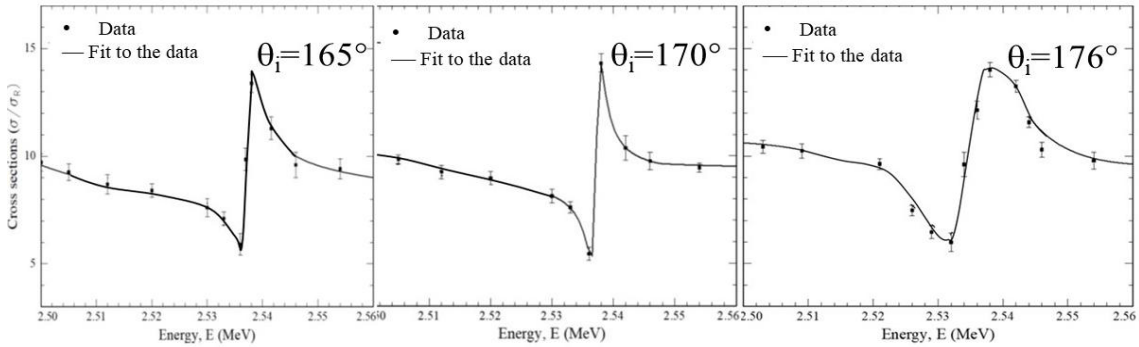

Figure 6. Spectra of the $^{14}N(p, p_0)^{14}N$ cross-sections at angles 165°, 170° and 176°, in the energy range 2440 to 2500 keV for the spin parity of J^{π} of $3/2^{-}$. Γ was 10±2 keV. E_r for the reactions was 2520±18 keV.

The cross-sections presented in this study are relatively higher than those of the various authors that are contained in the IBANDL nuclear data library [28]. N is a principal element in amino acids and therefore in proteins; most protein consists of a minimum of 200 amino acids. Thus, with these new cross-sections the researcher should obtain results of an improve accuracy.

4. CONCLUSION

There should definitely be a concern in the use of cross-sections data when determining the concentrations of elements that are cardinal to the composition of the specimen, especially so nitrogen. It was found in this study that existing discrepancies in the

experimental cross sections were relatively high when comparing data that were obtained at nearly the same backscattering angles. A new set of cross-sections were presented. It is recommended the cross-section should especially be applied in the cases where characterization of biomedical tissues are needed.

REFERENCES

[1] Mayer, J.W., Rimini, E., *Ion beam handbook for material analysis*, Elsevier, 2012.
[2] Nastasi, M., Mayer, J.W., Wang, Y., *Ion beam analysis: fundamentals and applications*, CRC Press, 2014.
[3] Rauhala, E., *Nuclear Instruments and Methods in Physics Research: Section B* **12**, 447, 1985.
[4] Mars, J.A., *Applications of the nuclear microprobe in materials science*. Doctorate of Technology Thesis: Cape Peninsula University of Technology, Bellville, Rep. of South Africa, 2004.
[5] Johansson, S., Campbell, J., Malmqvist, K., Winefordner, J., *Particle-induced X-ray emission spectrometry* (PIXE), John Wiley & Sons, 1995.
[6] Ishii, K., Morita, S., *Nuclear Instruments and Methods in Physics Research: Section B*, **34,** 209, 1988.
[7] Prozesky, V., Przybylowicz, W., Van Achterbergh, E., Churms, C., Pineda, C., Springhorn, K., Pilcher, J., Ryan, C., Kritzinger, J., Schmitt, H., *Nuclear Instruments and Methods in Physics Research: Section* B, **104**, 36, 1995.
[8] Hagedorn, F., Mozer, F., Webb, T., Fowler, W., Lauritsen, C., *Physical Review*, **105**, 219, 1957.
[9] Olness, J.W., Vorona, J., Lewis, H.W., *Physical Review*, **112**, 475, 1958.
[10] Bashkin, S., Carlson, R., Douglas, R., *Physical Review*, **114**, 1552. 1959.
[11] Ferguson, A., Clarke, R.L., Gove, H.E., *Physical Review*, **115**, 1655, 1959.
[12] Lambert, M., Durand, M., *Physics Letters* B, **24**, 287, 1967.
[13] Guohua, Y., Dezhang, Z., Hongjie, X., Haochang, P., *Nuclear Instruments and Methods in Physics Research: Section B*, **61**, 175, 1991.
[14] Havránek, V., Hnatowicz, V., Kvítek, J., *Czechoslovak Journal of Physics*, **41**, 928, 1991.
[15] Ramos, A., Paúl, A., Rijniers, L., da Silva, M., Soares, J., *Nuclear Instruments and Methods in Physics Research*: *Section B*, **190**, 95, 2002.
[16] Jiang, W., Shutthanandan, V., Thevuthasan, S., Wang, C.M., Weber, W.J., *Surface and Interface Analysis*, **37**, 374, 2005.
[17] Gurbich, A., *Sigmacalc*. http://www-nds.iaea.org/sigmacalc, 2010.
[18] Berthier, B., Berthoumieux, E., Gallien, J., Moreau, C., Raoux, A., *Nuclear Instruments and Methods in Physics Research*: *Section B*, **130**, 224, 1997.
[19] Berthoumieux E., Berthier B., Moreau, C., Gallien, J., Raoux, A., *Nuclear Instruments Methods in Physics Research*: *Section B*, **136**, 55, 1998.
[20] Berthoumieux, E., *Nuclear Physics* A, **758**, 118. 2005.
[21] Lane, A., & Thomas, R., *Reviews in Modern Physics*, **30**, 257, 1958.
[22] de Boer, R. J., Bardayan, D.W., Göorres, J., LeBlanc P., Manukyan K.V. Moran M.T., Smith K., Tan W., Uberseder E., Wiescher M., Bertone P.F., Champagne A.E. & Islam. M.S, *Physics Review C*, **91**, 045804, 2015.
[23] Gurbich, A., *Nuclear Instruments and Methods in Physics Research*: *Section B*, **261**, 401, 2007.
[24] Ajzenberg-Selove, F., *Nuclear Physics A*, **449**, 1, 1986.
[25] Kuisma-Kursula, P., *X-Ray Spectrometry: An International Journal*, **29**(1), 111, 2000.
[26] Tirira, J., Serruys, Y., Trocellier, P., *Forward recoil spectrometry: Applications to hydrogen determination in solids*, Vol. 163, Plenum Press. 1996.
[27] IBANDL *Ion Beam Analysis Nuclear Data Library*, Internet Access: https://www-nds.iaea.org/exfor/ibandl.htm, accessed March, 13th, 2019.